20th IMEKO TC4 International Symposium and
18th International Workshop on ADC Modelling and Testing
Research on Electric and Electronic Measurement for the Economic Upturn
Benevento, Italy, September 15-17, 2014

A magnetic current sensor with SQUID readout

Luca Callegaro[1], Bruno Trinchera[1], Luca Roncaglione Tet[1]

[1]*INRIM - Istituto Nazionale di Ricerca Metrologica, Torino, Italy*

***Abstract* – A cryogenic magnetic current sensor has been constructed and tested for operation and sensitivity in the ac regime. The sensor is based on a ferromagnetic-core current transformer, coupled to a superconducting-quantum-interference-device (SQUID) current detector. The SQUID electronics provides a voltage output that can be coupled to room temperature signal recovery electronics, such as a lock-in amplifier. Working in liquid helium ($4.2\,\mathrm{K}$) the sensor transresistance is about $1.8\,\mathrm{M\Omega}$ in the audio frequency range; the equivalent input current noise of the sensor, at the frequency of $1\,\mathrm{kHz}$, is a few $\mathrm{pAHz}^{-1/2}$ per unit primary winding turn. A major contribution to the detector noise is the thermal noise of the ferromagnetic core; however, an important excess noise contribution at low frequency is also present. The experiment is intended as a feasibility test towards the realization of high-sensitivity electromagnetic devices, such as current comparators, to be employed in primary current and impedance metrology setups working in the audio frequency range.**

I. INTRODUCTION

The application of magnetic sensing of electrical currents is ubiquitous in test and measurement applications [1, 2]. In the field of electrical metrology, current transformers and current comparators allow the precise measurement of both dc and ac currents and of current ratios, and constitute a pillar of electrical impedance metrology [3, Sec. 4.5].

Current comparators (CC) [4] are the most accurate current ratio standards available. They reach uncertainties better than parts in 10^6, both in dc and in the audio frequency range. In a CC, a ferromagnetic core defines a closed flux path of high permeability $\mathcal{P}$. The currents I_k to be compared flow through windings of n_k turns, linked to the core. The resulting magnetomotive force $\mathcal{M} = \sum n_k I_k$ generates a magnetic flux $\Phi = \mathcal{P}\mathcal{M}$. In the ac regime, Φ is sensed by a suitable detection winding, connected to the input of a front-end amplifier and signal-recovery electronics. In the dc regime, Φ is sensed with fluxgate techniques [2, 5]. If the condition $\Phi = 0$ occurs, then $\sum n_k I_k = 0$, and the current ratio is equal to the turns ratio.

The sensitivity of a CC is limited by the noise occurring in the detection of the condition $\Phi = 0$. If the noise of I_k can be neglected, the detection noise is caused by the spontaneous fluctuations of Φ in the ferromagnetic core employed, and by the noise of the signal conditioning electronics (which is in turn typically associated with that of its front-end amplifier). A CC working in a cryogenic environment benefits of a reduction of all noise contributions caused by thermal fluctuations, and of the possibility of using the extremely sensitive superconducting-quantum-interference devices (SQUID) as flux detector.

We realized a cryogenic magnetic current detector provided with a SQUID front-end electronics. The paper reports on measurements performed with the detector and its noise in the audio frequency bandwidth. The experiment is to be intended as a feasibility test towards the realization of a cryogenic current comparator (CCC; see [6] and references therein) working in ac regime [7–12]

II. EXPERIMENTAL

A schematic view of the experimental system is shown in Fig. 1.

A small $1:1$ current transformer is constructed with a primary and a secondary winding, both having 1 turn, and made of non-superconducting metal (enameled copper) wound on a ferromagnetic core. Actually, two equal cores (Vacuumschmelze VITROPERM 500 F, model T60006-L2016-W403-04 toroidal core, $16\,\mathrm{mm}$ outside diameter, $10\,\mathrm{mm}$ inside diameter, $6\,\mathrm{mm}$ height) have been employed, wound in opposite directions in order to minimize the magnetic coupling with possible external magnetic interference sources. No superconducting shielding of the core or the windings has been employed.

The SQUID [13] is a wideband commercial model, a Magnicon 1-stage SQUID current sensor C6XXL1W. Its main specifications are:

- nominal input inductance $L_{\text{SQUID}} = 1.8\,\mathrm{\mu H}$;
- input coupling $1/M_{\text{in}} = 0.232\,\mathrm{\mu A}\,{\Phi_0}^{-1}$, where $M_{\text{in}} = 8.914\,\mathrm{nH}$ is the mutual inductance between the input coil and the Josephson junction loop;
- transfer coefficient[1] $V_\Phi = 580.7\,\mathrm{\mu V}\,{\Phi_0}^{-1} = 280.8\,\mathrm{GHz}$

[1]The quantity $\Phi_0 = h/2e = 2.067\,833\,667(52) \times 10^{-15}$ Wb [14] is the magnetic flux quantum. h is the Planck constant, e the elementary charge.

ISBN-14: 978-92-990073-2-7

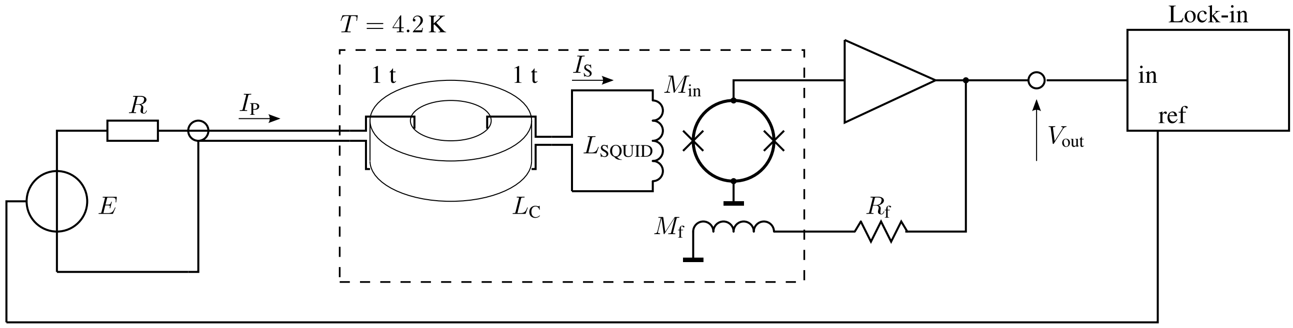

Fig. 1. Schematic representation of the experiment. A voltage source E and a high-valued resistor R constitute a low current source I_{P}. The current is injected in the one-turn primary winding of the ferromagnetic current transformer. The secondary winding, having an output inductance L_{C}, is coupled to the SQUID input (having inductance L_{SQUID}). The magnetic flux generated by I_{S} is coupled to the SQUID via the mutual inductance M_{in}. The SQUID is read by a sensitive integrative voltage amplifier, which output V_{out} can be read by the lock-in amplifier or by a signal analyzer (not shown). The voltage V_{out}, through a feedback resistance R_{f} and a feedback mutual inductance M_{f}, holds the flux in the SQUID to zero (within a multiple of the flux quantum Φ_0).

- feedback sensitivity $1/M_{\mathrm{f}} = 42.6\,\mu\mathrm{A}\,{\Phi_0}^{-1}$, where $M_{\mathrm{f}} = 48.54\,\mathrm{pH}$ is the mutual inductance between the feedback coil and the Josephson junction loop;
- flux noise $S_{\Phi}^{\mathrm{SQUID}} = 0.937\,\mu\Phi_0\mathrm{Hz}^{-1/2} = 1.94 \times 10^{-21}\,\mathrm{WbHz}^{-1/2}$ at the frequency of $1\,\mathrm{kHz}$.

The SQUID is enclosed in a Nb superconducting capsule and is operated with its room-temperature electronics (Magnicon XXF-1), which achieves a $50\,\mathrm{MHz}$ open-loop bandwidth and a $20\,\mathrm{MHz}$ flux-locked-loop bandwidth.

The current transformer and the SQUID are mounted at the end of a cryogenic probe, provided with a magnetic shield made of a thin $\mu-$metal foil, and with coaxial leads to the room-temperature environment. The SQUID is constructed to allow cooling under the Earth magnetic field, and no further magnetic shielding has been found necessary for its proper working. A photo of the cryogenic probe head is shown in Fig. 2.

During operation, the probe is inserted in a liquid helium dewar at ambient pressure, reaching a working temperature $T = 4.2\,\mathrm{K}$. The SQUID is operated in flux-locked-loop configuration (see the caption of Fig. 1), in order to achieve a linear response. A feedback resistance $R_{\mathrm{f}} = 10\,\mathrm{k}\Omega$ is employed during all experiments.

The primary winding can be fed with a test current I_{P}, generated with a commercial voltage waveform synthesizer E and a high-valued resistor R in series. R has a nominal value of $10\,\mathrm{M}\Omega$ and has been calibrated in the audio frequency range. The secondary current $I_{\mathrm{S}} \approx I_{\mathrm{P}}$ is directly connected to the SQUID input. The voltage output of the SQUID electronics is measured either with a fast-fourier-transform (FFT) signal analyzer (Agilent mod. 34970A), or with a lock-in amplifier (Stanford Research mod. 830), phase-locked to the synthesizer with a reference signal.

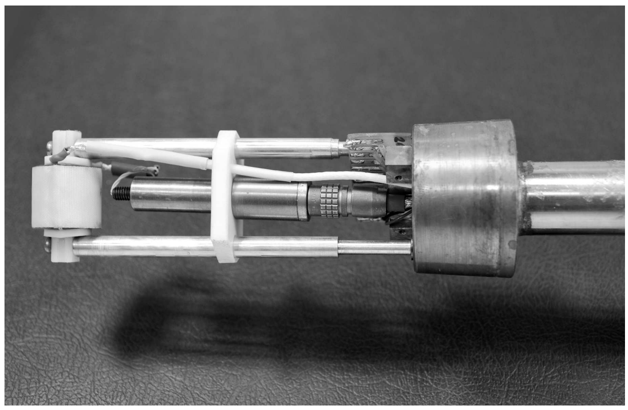

Fig. 2. Photo of the cryogenic probe head. On the left, the magnetic core with the primary and secondary windings, wrapped in Teflon tape. In the center, the SQUID, enclosed in a cylindrical Nb superconducting capsule fixed on a Teflon plate. The probe holder on the right is a stainless steel thin-walled tube, whitin all wirings to the room-temperature environment are located.

III. RESULTS

A. Transformer characterization

The equivalent inductance L_{C} and resistance R_{C} per unit winding turn, has been determined at the working temperature $T = 4.2\,\mathrm{K}$ by performing impedance measurements (with an LCR meter) on a larger core of the same material, wound with 70 turns, and by scaling the measured values accordingly. At the center frequency of $1.592\,\mathrm{kHz}$ ($\omega = 10\,\mathrm{krad\,s}^{-1}$), $L_{\mathrm{C}} \approx 56\,\mu\mathrm{H}$, which is mismatched to the specified SQUID input inductance $L_{\mathrm{SQUID}} = 1.8\,\mu\mathrm{H}$. In order to further improve the potential sensitivity, fractional-turn loop techniques [15] could be considered in the future.

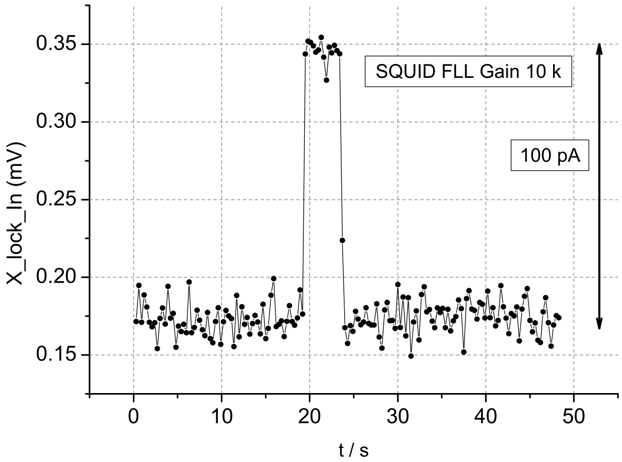

Fig. 3. Time series of lock-in readings of the voltage generated by the SQUID electronics. A step $I_\mathrm{P} = 100\,\mathrm{pA}$ is applied for an interval of time (a few seconds) during the recording.

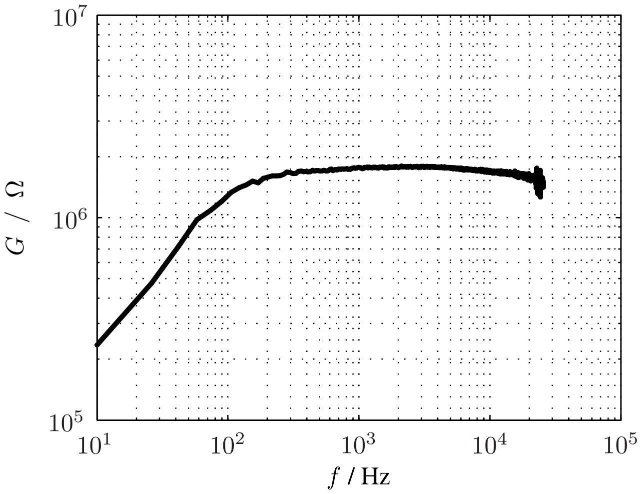

Fig. 4. Transresistance gain G of the magnetic current sensor, measured with the FFT signal analyzer and a white noise signal excitation.

B. Signal detection

A first series of measurements has been performed by driving the system with a sinusoidal excitation E and sampling the lock-in amplifier readings. Fig. 3 shows a time series of sampled magnitude readings of the lock-in amplifier at $f = 1.592\,\mathrm{kHz}$; during the acquisition, a current test signal $I_\mathrm{P} = 100\,\mathrm{pA}$ is generated.

C. Gain and noise

A second series of measurements have been performed with the FFT signal analyzer connected to the SQUID electronics output. The FFT analyzer can perform gain/phase analysis, or spectral analysis.

The transresistance gain of the magnetic current sensor $G = V_\mathrm{out}/I_\mathrm{P}$ has been measured with the analyzer in correlation mode, using a white noise signal excitation for E. The result is shown in Fig. 4. At low frequency the cutoff is caused by the ac coupling of the electronic chain. Above the frequency cutoff around $100\,\mathrm{Hz}$, G is approximately constant. Its value is consistent with the theoretical gain G^SQUID of the SQUID sensor and its electronics, which can be calculated from its specifications as

$$G^\mathrm{SQUID} = \frac{M_\mathrm{in}}{M_\mathrm{f}} R_\mathrm{f} = 1.84\,\mathrm{M\Omega}. \tag{1}$$

The output voltage noise is measured with the FFT analyzer in spectrum analysis mode. Together with the measured gain $G(f)$, it is possible to estimate the equivalent current noise power spectral density $S_\mathrm{I}(f)$ at the primary winding input, which is shown in Fig. 5.

IV. DISCUSSION

The sources of detection noise S_I are:

- the flux noise of the ferromagnetic core. The equilibrium thermal noise caused by flux thermal fluctuations can be evaluated with the Johnson-Nyquist theorem [16–18] from electrical impedance measurements. One can write $S_\mathrm{I}^\mathrm{th}(f) = 4k_\mathrm{B}T\,G_\mathrm{C}(f)$, where G_C is the equivalent conductance of the secondary winding. Fig. 5 shows the result of the calculation. The behavior of the thermal noise spectrum, and in particular its $1/f$ behavior at low frequencies, is consistent with previous observations, see e.g. [19].

- the intrinsic flux noise of the SQUID. It can be calculated as $S_\mathrm{I}^\mathrm{SQUID} = S_\Phi^\mathrm{SQUID}/M_\mathrm{in} = 1.87 \times 10^{-13}\,\mathrm{A\,Hz^{-1/2}}$, and can therefore can be considered negligible in this experiment.

- the noise of the SQUID electronics, of the FFT analyzer, the thermal noise of the wiring and of the electrical components connected to the primary winding, and the electromagnetic interferences from the outside. These contributions can be considered negligible in this experiment.

Fig. 5 allows to compare the measured S_I with the calculated $S_\mathrm{I}^\mathrm{th}(f)$. The comparison shows that S_I diverges from S_I^th at low frequency, and an excess noise is present. Such behavior will be investigated in the future: a probable cause is the presence of slow relaxations toward equilibrium of the residual dc magnetization of the core.

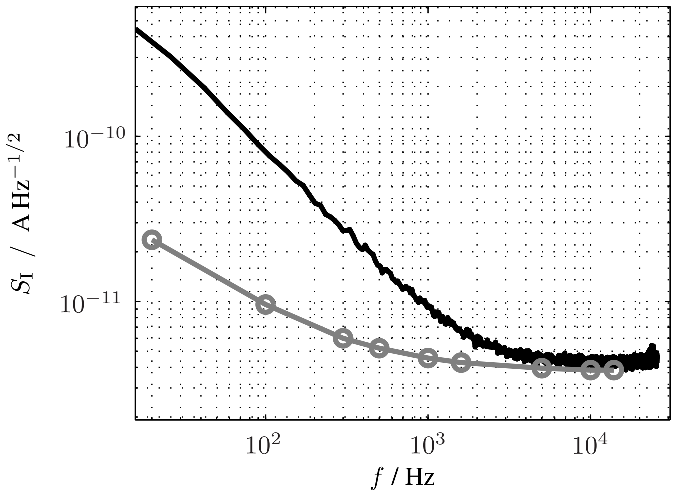

Fig. 5. (black) Equivalent current noise spectral density S_{I} at the primary winding input. (gray) Thermal noise of the ferromagnetic core $S_{\mathrm{I}}^{\mathrm{th}}(f)$, calculated with the Johnson-Nyquist theorem starting from the equivalent conductance measurement of the secondary winding G_{C} and an environmental temperature $T = 4.2\,\mathrm{K}$.

V. CONCLUSIONS

The experiments confirm the feasibility of low-noise cryogenic magnetic current detectors, based on ferromagnetic-core elements and coupled to SQUID electronics, suitable for operation in the audio frequency range.

The measured noise of the realized device, of $6\,\mathrm{pAHz}^{-1/2}$ per unit primary winding turrn at $1.592\,\mathrm{kHz}$, can be compared for example with the measured current noise of $82\,\mathrm{pAHz}^{-1/2}$ per unit turn that we measured on a room-temperature CC [20] with the same core material but a much larger core size (about 10 times the cross section).

The origin of the detector noise can only in part be traced back to the thermal noise from the ferromagnetic core: an unexpected low-frequency excess noise is also present. It is likely that both noise contributions can be improved by a proper choice of ferromagnetic core material [21] and cooling and demagnetizing procedures.

The noise level is of interest for the realization of low-noise electromagnetic devices, such as ac cryogenic current comparators, suitable for primary impedance comparisons. These devices will also benefit of the use of superconducting shields for the suppression of ratio errors of magnetic origin [6].

VI. ACKNOWLEDGMENTS

The authors are indebted with Cristina Cassiago and Matteo Fretto, INRIM, for help in the setup of the cryogenic conditions for the experiment. The activity has been partially financed by Progetto Premiale MIUR-INRIM P6-2012 *Implementation of the new International System (SI) of Units*. The work has been realized within the European Metrology Research Programme (EMRP) Project SIB53 AIM QuTE, *Automated impedance metrology extending the quantum toolbox for electricity*. The EMRP is jointly funded by the EMRP participating countries within EURAMET and the European Union.

REFERENCES

[1] P. Ripka, "Current sensors using magnetic materials," *J. Optoelectron. and Adv. Materials*, vol. 6, pp. 587–592, Jun 2004.

[2] ——, "Electric current sensors: a review," *Meas. Sci. Technol.*, vol. 21, p. 112001, 2010, 23 pp.

[3] L. Callegaro, *Electrical impedance: principles, measurement, and applications*, ser. in Sensors. Boca Raton, FL, USA: CRC press: Taylor & Francis, 2013, iSBN: 978-1-43-984910-1.

[4] W. J. M. Moore and P. N. Miljanic, *The current comparator*, ser. IEE electrical measurement series. London, UK: P. Peregrinus Ltd, 1988, vol. 4, iSBN 0-86341-112-6.

[5] M. P. MacMartin and N. L. Kusters, "A direct-current-comparator ratio bridge for four-terminal resistance measurements," *IEEE Trans. Instr. Meas.*, vol. 15, no. 4, pp. 212 –220, Dec 1966.

[6] J. M. Williams, "Cryogenic current comparators and their application in electrical metrology," *IET Sci. Meas. Technol.*, vol. 5, no. 6, pp. 211–224, 2011.

[7] K. Grohmann, H. D. Hahlbohm, H. Lübbig, and H. Ramin, "Current comparators with superconducting shields," *Cryogenics*, pp. 499–502, Sep 1974.

[8] ——, "Ironless cryogenic current comparator for AC and DC applications," *IEEE Trans*, vol. IM-23, no. 4, pp. 261–263, Dec 1974.

[9] K. Grohmann and D. Hechtfischer, "Self-calibrating cryo current comparators for AC applications," *IEEE Trans. Instr. Meas.*, vol. IM-33, no. 2, pp. 91–96, 1984.

[10] H. Seppä, A. Satrapinski, T. Varpula, and J.-M. Saari, "Frequency dependence of 100 Ω standard resistors measured with a CCC-based AC resistance bridge," *IEEE Trans. Instr. Meas.*, vol. 44, no. 2, pp. 276–280, 1995.

[11] H. Seppä and A. Satrapinski, "AC resistance bridge based on the cryogenic current comparator," *IEEE Trans. Instr. Meas.*, vol. 46, no. 2, pp. 463–466, Apr 1997.

[12] H. Seppä, A. Satrapinksi, M. Kiviranta, and V. Virkki, "Thin-film cryogenic current comparator," *IEEE Trans. Instr. Meas.*, vol. 48, no. 2, pp. 365–369, Apr 1999.

[13] D. Drung, C. Assmann, J. Beyer, A. Kirste, M. Peters, F. Ruede, and T. Schurig, "Highly sensitive and

easy-to-use SQUID sensors," *IEEE Trans. Appl. Supercond.*, vol. 17, no. 2, pp. 699–704, Jun 2007.

[14] P. J. Mohr, B. N. Taylor, and D. B. Newell, "CODATA recommended values of the fundamental physical constants: 2010," *Rev. Mod. Phys.*, vol. 84, no. 4, pp. 1527–1605, 2012.

[15] J. Sesé, A. Camón, C. Rillo, and G. Rietveld, "Ultimate current resolution of a cryogenic current comparator," *IEEE Trans. Instr*, vol. 48, no. 6, pp. 1306–1313, Dec 1999.

[16] J. B. Johnson, "Thermal agitation of electricity in conductors," *Phys. Rev.*, vol. 32, pp. 97–109, Jul. 1928.

[17] H. Nyquist, "Thermal agitation of electric charge in conductors," *Phys. Rev.*, vol. 32, pp. 110–113, Jul. 1928.

[18] H. B. Callen and T. A. Welton, "Irreversibility and generalized noise," *Phys. Rev.*, vol. 83, pp. 34–40, Jul 1951.

[19] G. Durin, P. Falferi, M. Cerdonio, G. A. Prodi, and S. Vitale, "Low temperature properties of soft magnetic materials: magnetic viscosity and $1/f$ thermal noise," *J. Appl. Phys*, vol. 73, no. 10, pp. 5363–5365, 15 May 1993.

[20] B. Trinchera, V. D'Elia, and L. Callegaro, "A digitally assisted current comparator bridge for impedance scaling at audio frequencies," *IEEE Trans. Instr. Meas.*, vol. 62, no. 6, pp. 1771–1775, 2013.

[21] R. Geithner, D. Heinert, R. Neubert, W. Vodel, and P. Seidel, "Low temperature permeability and current noise of ferromagnetic pickup coils," *Cryogenics*, vol. 54, pp. 16 – 19, 2013.